Biochemical and Biophysical Research Communications **271,** 170–180 (2000)
doi:10.1006/bbrc.2000.2595, available online at http://www.idealibrary.com on IDEAL®

Differential Expression of Sense and Antisense Transcripts of the Mitochondrial DNA Region Coding for ATPase 6 in Fetal and Adult Porcine Brain: Identification of Novel Unusually Assembled Mitochondrial RNAs

Uwe Michel,*[,1] Argyrios K. Stringaris,*[,1] Roland Nau,* and Peter Rieckmann†
**Laboratory of Neurobiology, Department of Neurology, University of Göttingen, Robert-Koch-Strasse 40, 37075 Göttingen, Germany; and †Clinic of Neurology, Kopfklinikum, University of Würzburg, Josef-Schneider-Strasse 11, 97078 Würzburg, Germany*

Received February 12, 2000

The mammalian mitochondrial genome is a double-stranded circular DNA molecule, which is transcribed from both strands as polycistronic RNAs, which are further processed to yield the mature polyadenylated mRNAs, rRNAs and tRNAs. We compared the gene expression patterns of foetal and adult porcine brains and identified a sequence tag from the ATPase 6 region of the mitochondrial genome which, in adult brain, was more abundant in the sense (H-strand) form, but, in foetal brain, more abundant in the antisense form (L-strand). By means of solution hybridisation/S1 nuclease protection assay, Northern blotting, and PCR based techniques, we demonstrated that the ATPase 6 region of the porcine mitochondrial genome is transcribed as co-existing, stable sense and antisense RNAs. Furthermore, we identified sense and antisense transcripts from this region consisting of inversely assembled fragments joined together at a direct repeat of 7 nucleotides. Our results suggest that transcription and post-transcriptional processing of mitochondrial RNAs are much more complex than presently thought.

Normal brain function depends upon adequate levels of energy supplies, and it has been shown that even subtle alterations in mitochondrial function can lead to insidious pathological changes in neurons (1–3). Since the discovery of pathogenic mitochondrial DNA mutations (4, 5), the role of mitochondrial dysfunction in diverse neurological disorders has been studied intensively (DiMauro and Bonilla, 1997) (6, 7).

The mammalian mitochondrial genome is a highly organised double-stranded DNA molecule of about 16.5 Kbp encoding two rRNAs, 14 tRNAs and 12 mRNAs on the H-strand, and 8 tRNAs and one mRNA on the L-strand; it is attached to the inner mitochondrial membrane and not protected by proteins. The most striking characteristic of mitochondrial DNA is its extremely compact organisation (8, 9). All genes lack introns and are butt joined to each other or separated by very short nucleotide stretches. The economic organisation of mitochondrial DNA does not leave much space for intervening non-coding regulatory sequences. Transcription of both strands leads to the formation of polycistronic RNAs (10). Non-coding L-strand transcripts are short-lived and do not accumulate to a significant level in mitochondria (8, 11). The scattered distribution of tRNA genes, separating rRNA and protein-coding regions appears to function as a signal for RNA processing and maturation (12, 13). Although progress has been made to understand the regulation of RNA transcription in mitochondria, the exact mechanisms have not yet been completely elucidated. The involvement of transcription and post-transcriptional processing in the expression of the mitochondrial genome is evident from the observation that altered levels or incompletely processed transcripts correlate with mitochondrial diseases (14, 15). Furthermore, the identification of RNA transcripts superimposed to protein coding regions suggests that they might be involved in the control of mitochondrial gene expression (16–20).

In our effort to identify genes involved in the developmental processes of the brain, we compared the gene expression patterns of adult and foetal porcine brain tissues. During our studies we found a stable antisense transcript of the ATPase 6 region, which is differen-

[1] Both first authors contributed equally to the manuscript.

0006-291X/00 $35.00

tially expressed in foetal and adult brain. Furthermore, we provide evidence for RNAs from this region consisting of inversely aligned fragments. The fragments of these RNAs are joined together at a 7 nucleotides direct repeat and are transcribed from both, the L- and H-strand of the mitochondrial genome, they thus exist as sense and antisense transcripts.

MATERIALS AND METHODS

Materials. Materials were obtained from the following sources: ^{32}P-labelled nucleotides were from Nycomed Amersham (Amersham, UK). Reverse transcriptase and *Taq* polymerase from Gibco BRL (Grand Island, NY); oligonucleotides from NAPS (Göttingen, Germany); *Aspergillus oryzae* S1 nuclease from Nycomed Amersham (Amersham, UK); digoxigenin-labelled UTP, DIG Easy hybridisation solution, polyclonal antibody against digoxigenin (alaline phosphatase-conjugated), and the chemiluminescent substrate Disodium2-chloro5-(4-methoxyspiro{1,2′dioxetane-3,2′-(5′-chloro)[3.3.1.1] decan}-4/yl)-1-phenyl phosphate (CDP-Star) all from Boehringer Mannheim (Mannheim, Germany); the kit for cRNA synthesis was from Promega (Madison, WI).

Tissue sources and preparation of RNA. Porcine tissues from pregnant animals and their foetuses were generously provided by Drs. S. Wallenhorst and Dietrich (Institut für Tierzucht und Haustiergenetik; University of Göttingen) (21). Total RNA for Northern blotting, S1 nuclease analysis and differential display were prepared by the conventional guanidine isothiocyanate method (22).

Differential mRNA display (DD) and rapid amplification of cDNA ends (RACE). 50 μg of RNA from adult and foetal brain were digested with DNase, phenol/$CHCl_3$ and $CHCl_3$-extracted, precipitated and redissolved in RNase-free water. Reverse transcription was performed with 1–5 μg RNA and 1 μM of one degenerate downstream primer (23). The DD was essentially performed as originally described (23), except that each 5′ primer (10 mer) contained a restriction enzyme site and the 10-fold PCR buffer was 800 mM TRIS pH 8.9, 200 mM $(NH_4)_2SO_4$, 40 mM $MgCl_2$. For each radioactive PCR the equivalent of 0.2 or 0.02 μg of transcribed RNA was used in duplicate. The labelled PCR products were heated to 80°C for 3 min, transferred to ice water for 3 min and then separated on 6% non-denaturing acrylamide gels at 2400 V.

The cDNA bands of interest and their corresponding negative controls were cut from dried gels as described (23), with the minor change that the eluted cDNAs were not precipitated but recovered by lyophylisation. The dried pellets were resuspended in 15 μl water, and 3 μl were used for amplification in a 30 μl PCR. Non-radioactive PCR products from amplification of the specific band and their controls were run on 1.8% agarose gels together with size markers. The banding pattern between specific bands and control was compared to each other and to the original size estimation from the DD. In cases where the PCR products of the specific cDNA band and their negative controls were obviously different, the band(s) of proper size was/were transferred to and recovered from DEAE membranes (24); in cases where the amplification step of negative control and sample produced similar PCR products and where PCR products could not undoubtedly be assigned to the original size of the DD cDNA band, the whole PCR product was used for further cloning.

Unpurified PCR or PCR bands, which were eluted from DEAE membranes, were either digested with restriction enzymes according to the restriction enzyme site in the 3′ primer (see DD section) and then ligated into the appropriately cut pGEM4Z vectors, or cloned directly into pGEMT vector. The RACE was done with a Marathon cDNA Amplification kit from Clontech (Palo Alto, CA, USA) according to the instructions of the supplier. Resulting PCR products were cloned in pGEMT vector. Sequencing was performed with a T7 sequencing kit (Pharmacia, Freiburg, FRG) and later with a Big Dye Sequencing kit and an automatic sequencer from ABI Prism, Model 377.

S1 nuclease protection assay. S1 nuclease protection assay was performed as previously described (25). Part of our results were repeated with a modified form of this assay, which circumvents the problem of poor RNA solubility in high salt formamide buffers and loss of pellets during the isopropanol precipitation step. In brief, 20 μg of total RNA and, as negative controls, either 20 μg of yeast tRNA or 4 μg of porcine DNA were dissolved in 20 μl diethylpyrocarbonate (DEPC)-H_2O. 10 μl of 3-fold hybridisation buffer [75 mM PIPES (Piperazine-1,4-bis (2-ethanosulfonic acid))], pH 6.8; 600 mM NaCl; 3 mM EDTA) with 10^5 cpm of radioactively labelled cRNA probe were added to each sample. The samples were covered with mineral oil, denatured at 100°C for 5 minutes and then hybridised at 80°C for 3 h. Subsequently, 470 μl of S1 mix (50 mM NaCl; 30 mM Na-acetate, pH 4.6; 100 μg/ml herring sperm DNA; 4 mM $ZnSO_4$; 600 U/ml S1 nuclease) were added to each sample, and the digestion was performed at 37°C for 60 min. The digestion was stopped with 100 μl 4 M NH_4Ac/0.1 M EDTA. After precipitation with 10 μg yeast tRNA and 1 volume of isopropanol containing 35 μg/ml dextran blue, pellets were washed once with 70% ethanol and subsequently dissolved in 5 μl TE-buffer pH 8.0 [10 mM Tris · Cl (pH 8.0); 1 mM EDTA (pH 8.0)] and 4 μl loading buffer. Samples were heat denatured at 95°C for 3 min prior to loading on polyacrylamide gels containing 7 M urea. Autoradiography was performed on X-ray films with intensifying screens at −80°C or room temperature for varying time spans.

cRNA probes. After PCR reamplification of the original DD clone, the product was cloned in pGEMT vector. The clone contained a 162 bp fragment corresponding to nt 8020 to 8182 of the mitochondrial H-strand. A Sp6 cRNA transcript of the Nco I cut plasmid detected a 162 nt fragment of the mitochondrial H-strand transcript (DD antisense probe) in the S1 nuclease protection assay, and a T7 transcript of the Not I cut plasmid detected the corresponding 162 nt fragment of the mitochondrial L-strand transcript (DD sense probe). The RACE product was also cloned in pGEMT vector and is shown in detail in Fig. 5. cRNA transcribed with T7 polymerase from a Not I cut of the plasmid detected mitochondrial H-strand transcripts (RACE antisense probe), whereas the Sp6-derived cRNA from a Nco I cut of the plasmid detected mitochondrial L-strand transcripts (RACE sense probe); for some experiments a T7 transcript from a BsiW I cut was used to detect mitochondrial H-strand transcripts (BsiW I probe).

Analysis of in vitro forming double-stranded RNAs. Total RNA was heat-denatured at 95°C for 3 min and re-annealed by incubation with 3-fold hybridisation buffer at 65°C for 6 h. Following S1 nuclease digestion (see above), the samples were isopropanol-precipitated, pellets were washed in 70% ethanol and dissolved in 5 μl water. Then 25 μl of electrophoresis sample buffer [0.75 ml deionised formamide, 0.15 ml 10 × MOPS (3-*N*-morpholino propanesulfonic acid), 0.24 ml formaldehyde, 0.1 ml RNase-free water, 0.1 ml glycerol, 0.08 ml 10% (w/w) bromphenol blue] were added prior to further processing. Part of the samples were loaded on 1% non-denaturing agarose gels containing ethidium bromide, in order to assess complete digestion of 28 S and 18 S bands.

Northern analysis. Total RNA or S1-digested RNA hybrids were dissolved in 25 μl electrophoresis sample buffer. Samples were heated to 65°C for 15 min prior to loading on 1% denaturing agarose formaldehyde gels. The RNA was transferred onto Hybond N nylon membranes (Nycomed Amersham, Amersham, UK) in 20× SSC by capillary blotting overnight. In the case of DIG-labelled cRNA probes, the DIG-Easy hybridisation solution was used, and hybridisation proceeded at 68°C overnight. Hybridisation with radioactively labelled probes was performed overnight in a hybridisation solution containing 50% formamide; 25% 20× SSPE (175.3 NaCl:27,6 g $Na2HPO_4 · H_2O$; 7.4 g EDTA pH 7.4 per litre), 0.15 M

Tris–HCl pH 8; 1% SDS and 0.5% heparin (25000 U/ml) at 65°C: the hybridisation temperature for end-labelled oligonucleotides was 45°C. Membranes were washed under high stringency conditions in multiple steps. Filters hybridised with DIG-labelled cRNA probes were incubated with a polyclonal antibody against digoxigenin, conjugated to alkaline phosphatase. Detection was performed with the CDP-Star substrate according to the instructions of the supplier. Multiple film exposures with different time spans were obtained from each membrane.

RT-PCR analysis and primers. Reverse transcription reactions were performed with 5 μg total RNA. The RT primers were either 0.5 μg of random hexamers (Promega, WI), or 20 pmoles of specific primers. Primers were a 26-mer primer CATTGTTGGATCGAGATTGTGCGGTT (designated P1; nt 8085–8059, Accession No. AJ002189), reverse and complementary to the H- (sense) strand of mitochondrial DNA; a 21-mer primer GAGTCGTTTGGGTGTTGGGAA (designated P2; nt 8053–8033), reverse and complementary to the H- (sense) strand of mitochondrial DNA; a 23-mer primer (designated P3; nt 8179–8201), identical to the H-strand of mitochondrial DNA; a 23-mer primer CAGGTTTGGCCTTTTTGGTTGTG (designated P5; nt 8145–8123), reverse and complementary to the H-strand of mitochondrial DNA. Additional primers were the 38-mer CGTTTGGGTGTTGGGAATAGTAAATGTGATAAAAGCTG (designated P4a), reverse and complementary to the H-(sense) strand and spanning the 7 nucleotides overlap region of the RACE-clone and a 41-mer GCTTTTATCACATTTACTATTCCCAACACCCAAACGACTCA (designated P4s), reverse and complementary to the L-strand and spanning the 7 nucleotides overlap region; a 27-mer primer GGTTGTGAATAGCTATTATTTGTTTGG (designated P6; nt 8129–8103), reverse and complementary to the H-strand of mitochondrial DNA and a 24-mer primer CTACCACACTCATTCACACCCACC (designated P7; nt 8204–8227), corresponding to the H-strand of the mitochondrial DNA. PCR reactions were done with 20 pmol of each primers. For each PCR a 2 μl aliquot of the RT-reaction were used as a template. Annealing temperatures and $MgCl_2$ concentrations varied according to the primers and templates used.

Accession numbers. AF190812 for the unusually assembled transcripts and AF190813 for the ATPase 6/8 L-strand (antisense) transcript.

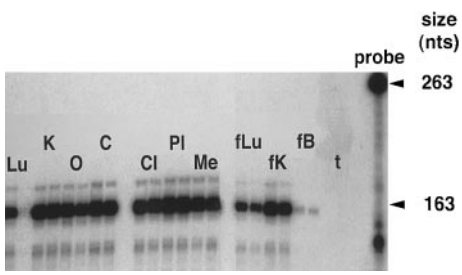

FIG. 1. Comparison of the steady-state levels of mitochondrial H-strand transcripts of the ATPase 6 region in multiple porcine tissues: Duplicates of 20 μg of total RNA from porcine lung (Lu), kidney (K), ovary (O), cerebrum (C), cerebellum (Cl), plexus choroideus (Pl), meninges (Me), foetal lung (fLu), foetal kidney (fK), foetal brain (fB), and 20 μg of yeast tRNA (t) were measured by solution hybridisation/S1 nuclease digestion assay with the ^{32}P-labelled DD antisense probe as described under Materials and Methods. The right-hand lane of the autoradiograph depicts the undigested probe, and the arrowheads with numbers indicate the sizes in nucleotides (nts) of the undigested probe (263) and of the protected fragments of the digested samples (163). The autoradiography was performed on X-ray film for 14 h at room temperature. (Please note that one of the duplicate pellets from adult lung was lost during the assay procedure.)

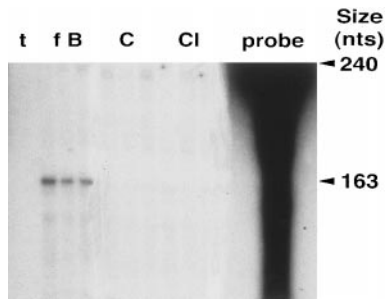

FIG. 2. Comparison of the steady-state levels of mitochondrial L-strand transcripts of the ATPase 6 region in foetal and adult porcine brain: foetal brain (fB), cerebrum (C) and cerebellum (Cl), yeast tRNA (t). From each sample 20 μg of total RNA were measured by solution hybridisation/S1 nuclease digestion assay with the ^{32}P-labelled DD sense probe as described under Materials and Methods. The right-hand lane of the autoradiograph depicts the undigested probe, and the arrowheads with numbers indicate the sizes in nucleotides (nts) of the undigested probe (240) and of the fragments of the digested samples (163). The autoradiography was performed on X-ray film with intensifying screens for 7 days at −80°C.

RESULTS

Stable L-Strand Transcripts of the ATPase 6 Region

The comparison of the gene expression patterns of adult and foetal porcine brains with differential display (DD) revealed, besides other bands which were specific for one of either tissue, one PCR fragment which was predominantly expressed in foetal brain and identical to porcine mitochondrial DNA from base pairs 8020 to 8182 (Accession No. AJ002189). This fragment corresponds to the ATPase 6 region of the porcine mitochondrial genome. The original up- and downstream primer for this RT-PCR were GCCCAAGCTT and T_{12}GC, respectively; the upstream primer matched the mitochondrial H-strand sequence by 90% and the anchor primer the L-strand sequence by 66%. To verify whether the difference in the RNA expression levels of the mitochondrial sequence seen in the DD corresponds to a real difference in mitochondrial RNA steady-state levels, we analysed the mitochondrial RNA expression level of foetal and adult brain tissue with sense and antisense cRNA probes derived from the DD clone by S1 nuclease protection assay.

In contrast to the original DD, we detected low levels of the H-strand transcripts in foetal brain, whereas high levels of H-strand expression were seen in adult cerebrum and cerebellum as well as in most other tissues (Fig. 1). The expression levels of the mitochondrial L-strand RNA were high in foetal brain but not in adult cerebrum and cerebellum (Fig. 2). The latter result was verified and extended by further tissue analyses using the DD sense probe. As shown in Fig. 3, the steady-state level of the mitochondrial L-strand transcript was the highest in foetal brain compared to all other foetal and adult tissues analysed. When foetal

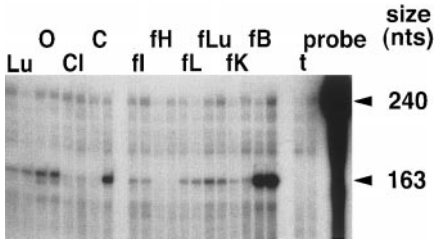

FIG. 3. Comparison of the steady-state levels of mitochondrial L-strand transcripts of the ATPase 6 region in multiple porcine tissues: lung (Lu), ovary (O), cerebellum (Cl), cerebrum (C), foetal intestine (fI), foetal heart (fH), foetal liver (fL), foetal lung (fLu), foetal kidney (fK), foetal brain (fB), and yeast tRNA (t). From each sample duplicates of 20 μg of total RNA were analysed by solution hybridisation/S1 nuclease digestion assay with the ^{32}P-labelled DD sense probe as described under Materials and Methods. The right-hand lane of the autoradiograph depicts the undigested probe, and the arrowheads with numbers indicate the sizes in nucleotides (nts) of the undigested probe (240) and protected fragments of the digested samples (163). The autoradiography was performed on X-ray film with intensifying screens for 14 days at −80°C. (Please note that one of the duplicate pellets from adult cerebrum was lost during the assay procedure.)

and adult brain tissues were compared, an inverse pattern of H- and L-strand transcripts was obvious from Figs. 1, 2, and 3.

We next performed Northern blottings with RNA from foetal brain and foetal muscle and used either the DD sense or the antisense cRNA probe, respectively, in order to determine the approximate sizes of the L- and H-strand transcripts. As can be seen in Fig. 4, the size of the L- (Fig. 4A) and major H- (Fig. 4B) strand transcript was the same (approximately 800 nucleotides [nts]). This is in accordance with reports on other species (26–28) and the expected size of 841 nts of the porcine ATPase 6/8 transcript (Accession No. AJ002189). In addition to the 800 bp H-strand transcript, 3 larger H-strand transcripts were detected with the DD antisense probe. In none of our Northern blots or S1 nuclease protection assays, neither tRNA from yeast nor DNA from porcine blood cells ever showed any cross-reactivity with the cRNA probes used.

Unusually Assembled Transcripts in the ATPase 6 Region

In an attempt to determine the 5′ end of the H- and L-strand transcripts, we performed 5′ RACE (rapid amplification of cDNA ends) with total RNA from porcine brain. PCR amplification of the H-strand RACE cDNA with primer P1 and the RACE anchor primer yielded one band of approximately 500 bp and occasionally a faint band of 1100 bp (data not shown). We only succeeded in subcloning the 500 bp product into pGEMT, and sequencing of the clone revealed a remarkable structure (Figs. 5A and 5B): Instead of having the mitochondrial sequence of the ATPase 6 region in a continuous order, the clone had a fragment of nt 8086 to nt 8526 (accession number AJ002189) joined directly to a fragment of nt 8027 to 8085 (Fig. 5A). The complete region of the cloned mitochondrial sequence encompasses nt 8027 to nt 8526 and is flanked by a perfect direct repeat of seven nucleotides at positions 8027–8033 and 8519–8526. This 7 nt direct repeat has the sequence TTACTAT and is the stretch where both fragments of the RACE clone overlap and join together (shaded area in Figs. 5A and 5B). Besides this, the RACE product had the P1 primer in an inverse order at the 3′ end, a structure which is most likely due to erroneous ligation of P1 primer during the RACE.

In order to prove that the unusually assembled mitochondrial transcript is a naturally occurring mitochondrial RNA of the H-strand and not a cloning artefact or a cloned fragment from mitochondrial DNA after a recombination event (29, 30), we performed S1 nuclease protection assays with total RNA from porcine brains. Figure 6 shows an S1 analysis of 20 μg of total RNA from foetal brain and tRNA with a labelled cRNA probe of 213 nts transcribed from the BsiW I cut RACE clone (Fig. 5B). The sizes of the three bands seen in Fig. 6 correspond well to the predicted protected fragments: the band with 161 nts represents the full-length fragment of the unusually assembled mitochondrial transcript, whereas the bands at 109 and 59 nts correspond to the fragments which result from hybridisation of the labelled cRNA to normal mitochondrial RNA.

The unusual structure of the assembled mitochondrial RNA urged us to use a third, independent experimental approach to confirm the results from the RACE and S1 nuclease protection assays. We therefore synthesised cDNA from foetal liver RNA with random hexamers and from adult cerebellum RNA with random hexamers and with primer P3. The resulting cDNAs were used for PCR with primers P3 and P2. The PCRs with the cDNAs synthesized with random hexamers yielded identical PCR products of approximately 370 bp, which, upon subcloning and sequencing, revealed a structure identical to the expected sequence encompassed by primers P2 and P3 in Fig. 5A; no PCR product was visible when water instead of cDNA was used as template. Due to the orientation of the primers, the PCR products could only have formed if the primer P2 and the random hexamer-primed cDNAs were derived from the unusually assembled H-strand transcript. Furthermore, cDNAs which were synthesised from foetal brain RNA with primers P1, P2 and random hexamers and which were amplified by PCR with primers P4 and P3 confirmed the above-described results and also yielded the expected products of approximately 370 bp (Fig. 7). Surprisingly, the PCR with cDNA derived from P3 primed cerebellum RNA and primers P2 and P3, which was performed as an addi-

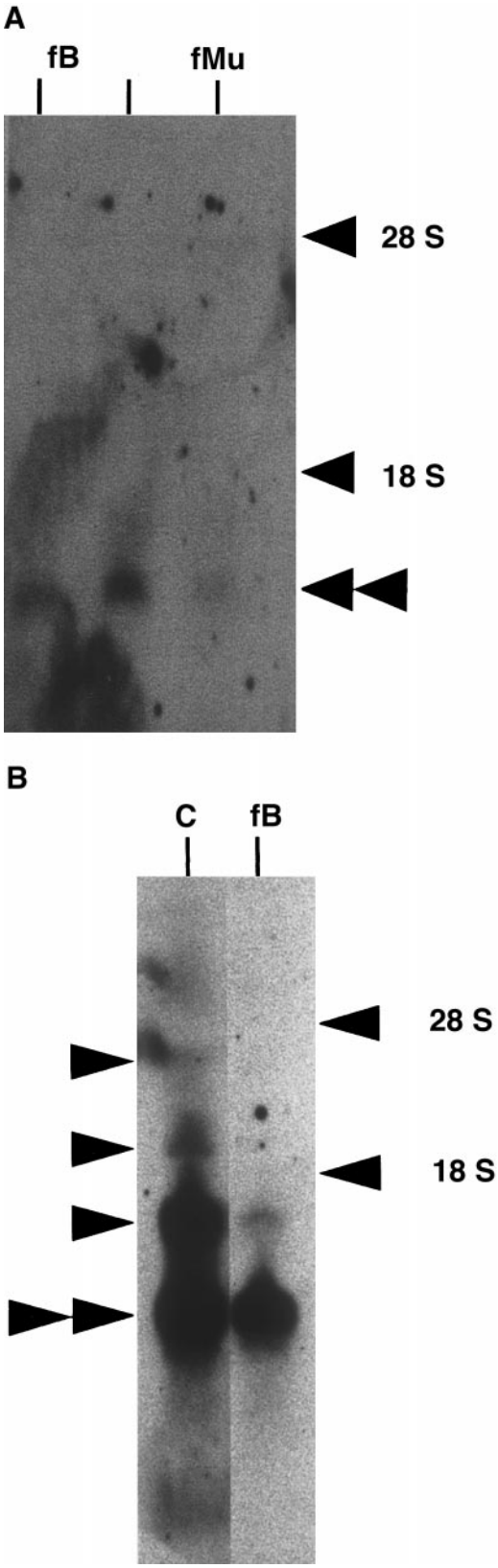

FIG. 4. Detection of mitochondrial L- and H-strand transcripts of the ATPase 6 region by Northern blotting. (A) 4 μg and 8 μg of total RNA from foetal brain (fB, lanes 1 and 2, respectively), and 7 μg of total RNA from foetal muscle (fMU, lane 3) were subjected to Northern blotting and L-strand transcripts were detected with a DIG-labelled sense DD probe as described under Materials and Methods. Arrowheads on the right side indicate the position of the 28S and 18S rRNA in comparison to the specific band of the mitochondrial L-strand transcript (double arrowhead). The estimated size of the L-strand transcript is approximately 800 nts. (B) 4 μg of total RNA from adult (C) and foetal brain (fB) were subjected to Northern blotting, and transcripts were detected with a DIG-labelled antisense DD probe. Arrowheads on the left side indicate the position of specific transcripts in comparison to the 28S and 18S rRNAs (arrowheads on the right side). The estimated sizes of the H-strand transcripts are approximately 800 nts (double arrowhead), 1600 nts, 2400 nts and 4800 nts.

tional negative control, also yielded the same product as the PCR with cDNA synthesised with random primers and primers P2 and P3. This result is unusual, since P3 can only bind to an L-strand sequence and thus pointed to the existence of an L-strand transcript, which is reverse and complementary to the unusually assembled H-strand transcript.

To confirm the PCR result of an unusually assembled L-strand transcript which is reverse and complementary to the already described H-strand transcript, we performed S1 nuclease protection assays with a labelled cRNA transcribed with Sp6 polymerase from the RACE clone; the cRNA probe would only bind to and thus protect the predicted unusually assembled L-strand transcript (Fig. 5B). Figure 8 shows a double band at approximately 490 nts in porcine cerebrum and foetal brain RNA but not in tRNA, which clearly demonstrates the occurrence of the unusually assembled mitochondrial L-strand transcript. The protected fragments were also seen with RNA from all other tissues tested (data not shown). As already demonstrated for the normal L-strand transcript with the DD sense probe (Figs. 2 and 3), the unusually assembled L-strand transcript also shows a higher expression in foetal than in adult brain (Fig. 8). However, the expression level of the unusually assembled H-strand transcript did not show reproducible differences between RNA preparations from foetal and adult brain (data not shown), as compared to those seen with the DD antisense probe (Fig. 1).

Double-Stranded Hybrid Formation of L- and H-Strand Transcripts

To prove the co-existence of stable L- and H-strand transcripts, total RNA from foetal brain was self-hybridised, treated with S1 nuclease to digest single-stranded RNAs and run on a Northern blot along with undigested RNA from foetal muscle and tRNA (see Materials and Methods). With the end-labelled antisense primer P4a, which spans the unusual assembly site of the RACE clone, the digested RNA from foetal brain revealed one major and one minor band; both

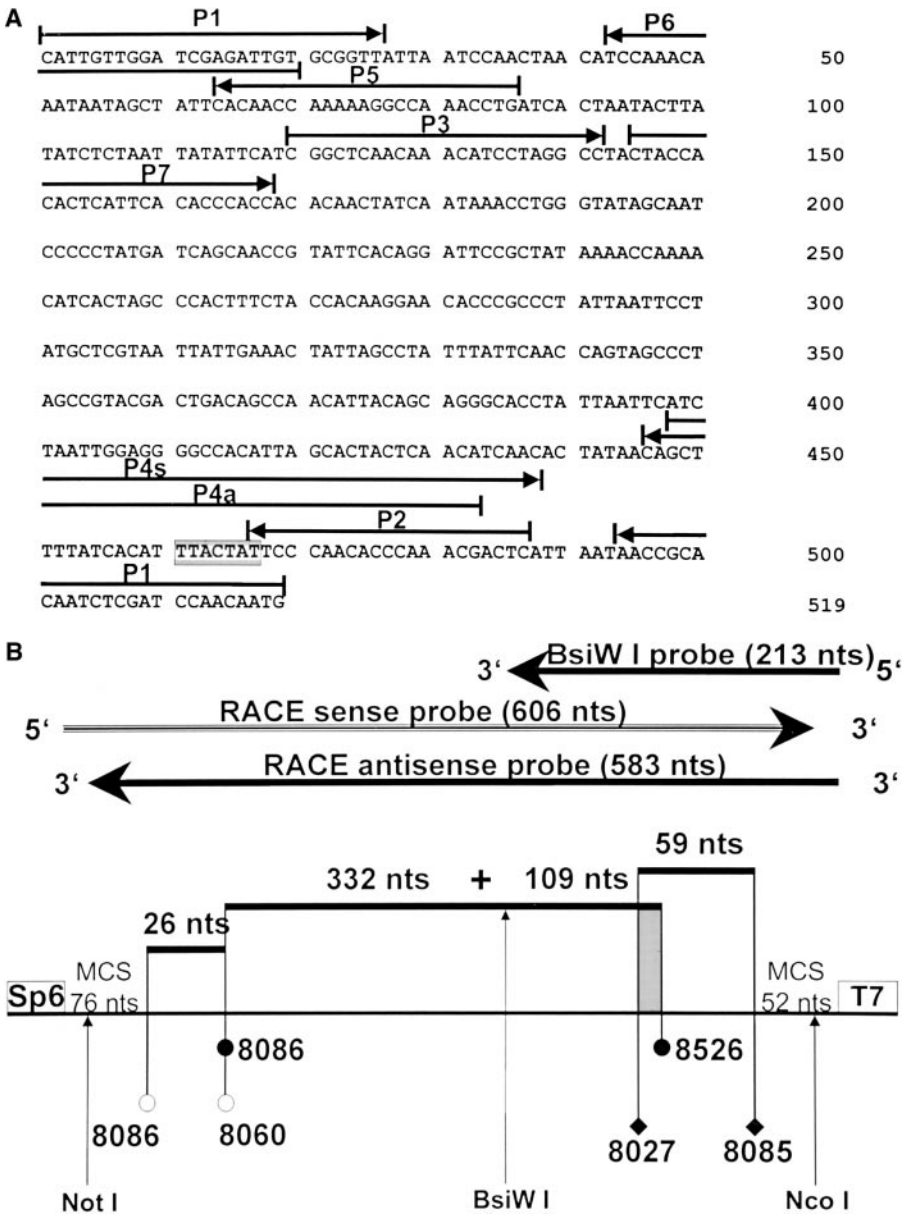

FIG. 5. Structure of the unusually assembled RACE clone in the mitochondrial ATPase 6 region. (A) Sequence of the unusually assembled H-strand transcript as determined by automatic sequencing. The arrows above the sequence, designated as P1 to P7, represent the primers used during the study. Arrows which point from 5′ to 3′ represent primers with the sequence as indicated (H-strand sequence), whereas arrows which point from 3′ to 5′ are reverse and complementary to the depicted sequence and correspond to the L-strand. The shaded area of 7 nts (TTACTAT) is the repeat, where the two fragments of the RACE clone overlap in an inverse order and which encompasses the amplified fragment in the original mitochondrial sequence at the 5′ end (nts 8027–8033 of AJ002189) and 3′ end (nts 8519–8526) (for further details, please refer to the text). (B) Schematic representation of the unusually assembled RACE clone in pGEMT vector and of the cRNA probes which derive from transcription of restriction enzyme cut (Not I, BsiW I, and Nco I, respectively) vectors by Sp6 and T7 polymerases. Numbers below the open and filled circles and below the filled squares correspond to the numbers of the genomic mitochondrial sequence (AJ002189) and refer to the 5′ and 3′ ends, respectively, of the fragments comprising the clone. Numbers above the bars indicate the sizes of the fragments in nucleotides (nts). The parts of the multiple cloning site (MCS) spanning from the transcription start sites to the respective beginning of the clone are also given in nts. The three arrows in the upper part of the cartoon represent the orientation and size of the sense and antisense cRNA probes used during this study.

bands correspond exactly in size to the bands detected with untreated RNA from foetal muscle (Fig. 9, upper panel). To demonstrate the complete digestion of the single-stranded RNAs in the foetal brain RNA samples, the blot was stripped and reprobed with an antisense cRNA probe of porcine GAPDH. Only the lane with the undigested RNA from foetal muscle showed the expected sized band for GAPDH RNA (Fig. 9, lower

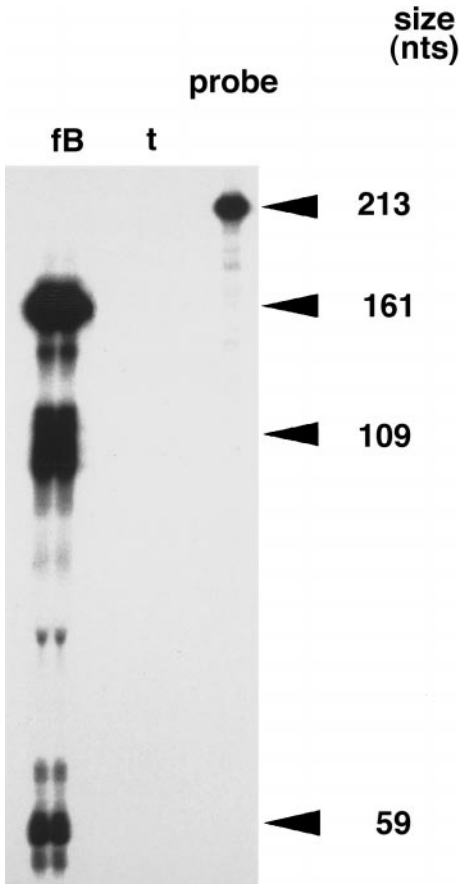

FIG. 6. X-ray autoradiograph of 20 μg of total RNA from foetal brain (fB) and 20 μg of yeast tRNA (t) as analysed by solution hybridisation/S1 nuclease digestion assay with an antisense cRNA probe derived from BsiW I cut plasmid. The right-hand lane of the autoradiograph shows the undigested probe, and the arrowheads with numbers indicate the sizes in nucleotides (nts) of the undigested probe (213) and the protected fragments derived from the digested samples (161, 109 and 59). The exposure time of the X-ray film was 10 h at −80°C.

panel); a parallel sample of S1-digested RNA analysed on an ethidium bromide-stained gel revealed no intact 28 S and 18 S RNA (data not shown).

In order to ascertain that the unusual transcripts detected by either end-labelled sense (primer P4s) or antisense (primer P4a) oligos in self-hybridised and S1 nuclease-digested RNA from foetal brain, have the same transcript size, digested and undigested RNA from foetal brain was analysed on Northern blots with either end-labelled primers P4s or P4a or with the antisense RACE cRNA probe. No differences in the sizes of the detected bands were observed, regardless of whether the RNA was derived from digested or undigested samples or which probe was used (Fig. 10). Northern blotting with the sense DD probe detected only one single band of approximately 800 bp (Fig. 4A). In contrast, when the labelled sense oligo (P4s) was used as probe, the 800 bp band and an additional bigger-sized band were detected in the digested samples (lanes 1 and 2 in Fig. 10 and Fig. 9); hardly any band was seen in the undigested RNA sample (lane 4 in Fig. 10). The antisense oligo P4a detected 3 bands in the digested samples. These 3 bands (lanes 5 and 6 in Fig. 10) and an additional bigger-sized band were detected by P4a in undigested RNA (lane 8 in Fig. 10). This pattern is identical to the Northern blot with the antisense DD (Fig. 4B) and to the pattern detected with the antisense RACE probe (lanes 9–12 in Fig. 10). The estimated sizes of the detected bands are approximately 800 nts, 1600 nts, 2400 nts and 4800 nts (Fig. 10).

DISCUSSION

The data presented above provide compelling evidence for the expression of a stable antisense transcript of the ATPase 6 region in many tissues. The

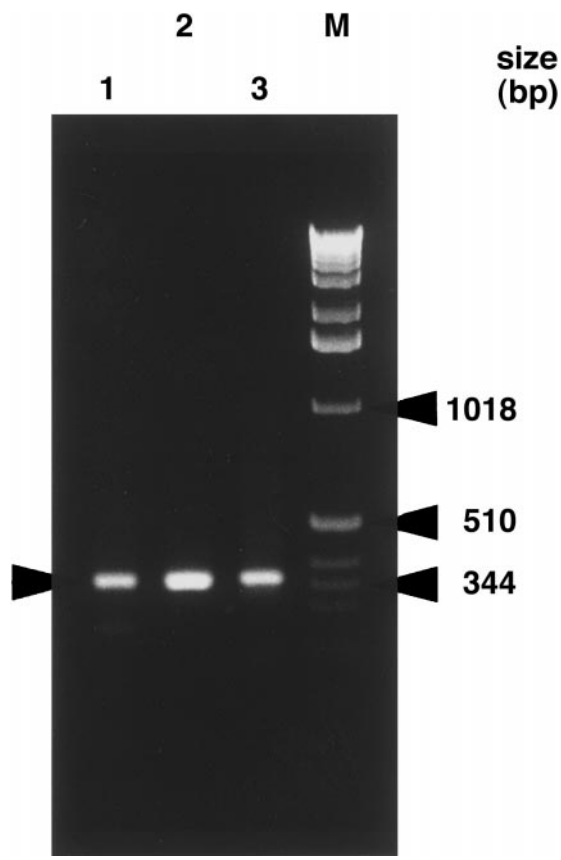

FIG. 7. Ethidium bromide-stained agarose gel of PCR products derived from amplification of cDNAs synthesised with primer P1 (lane 1), random primer (lane 2) and primer P2 (lane3) (see Fig. 5A for sequence) from total RNA of foetal brain. PCR primers were P4a and P3. The sizes of 3 bands from the molecular weight marker (M) are given in base pairs (bp) on the right side. The size of the PCR fragments is approximately 370 bp. Cycling conditions were: annealing at 65°C for 30 sec, denaturing at 95°C for 30 sec, and extension at 72°C for 2 min for 35 cycles.

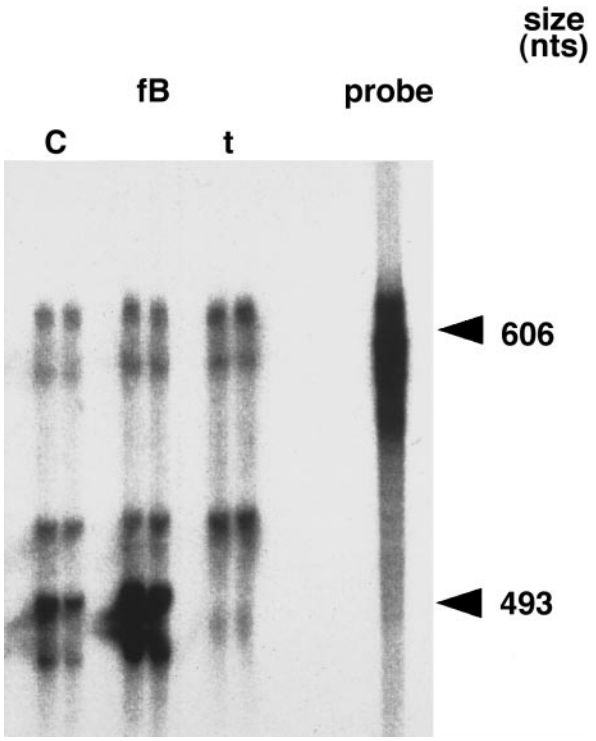

FIG. 8. X-ray autoradiograph of duplicates from 20 μg of total RNA from adult cerebrum (C) and foetal brain (fB) and 20 μg of yeast tRNA (t) as analysed by solution hybridisation/S1 nuclease digestion assay with a sense cRNA probe derived from the Nco I cut plasmid. The right-hand lane of the autoradiograph shows the undigested probe, and the arrowheads with numbers indicate the sizes in nucleotides (nts) of the undigested probe (606) and the protected fragment derived from the digested samples (493). The exposure time of the X-ray film was 3 days at −80°C.

steady-state level of this antisense RNA is regulated during brain development and is high in foetal but low in adult brain tissues; this pattern is inverse to the steady-state level of the H-strand transcript, which codes for ATPase 6 and 8 subunits. Furthermore, we demonstrate the expression of unusually assembled L- and H-strand-derived RNAs from the same region, which can form S1 nuclease-resistant double-stranded hybrids. These unusually assembled transcripts are composed of fragments which are joined together in an inverse order at a perfect direct 7 nts repeat. In Northern blottings with a cRNA probe derived from the usual ATPase 6 sequence, the unusually assembled transcripts cannot be distinguished from the usual ATPase 6/8 coding RNAs, because both transcripts reveal the same banding pattern. The transcripts can only be distinguished by S1 nuclease protection assay and are shown to co-exist.

The expression of the mitochondrial genome at the transcriptional level seems to be regulated by three strand-specific promoters (PH1, PH2, PL1) located in the D-(displacement) loop (10, 31) and by an attenuator sequence within the gene for the leucine-tRNA which is likely to account for the stoichiometric balance of rRNA to mRNA and a limited L-strand synthesis (32, 33). Subsequent to transcription, the polycistronic RNAs are mostly cleaved immediately 5′ and 3′ of a tRNA sequence (9, 12, 27, 34). Post-transcriptional events, such as polyadenylation and RNA degradation, then determine the stability of the individual transcription entities. The region of the mitochondrial genome, coding for the genes of the ATPase subunits 6 and 8 and the cytochrome C oxidase chain III (COIII), differs from the common scheme of individual genes separated by interspersed tRNA genes and is peculiar in two ways: no tRNA gene separates the genes of ATPase 6 and COIII (27), and the coding regions of ATPase 6 and 8 overlap (35–37) by 43 bp (in the pig). This raises the question of how the expression of the two ATPase subunits is coordinated and how the polycistronic tran-

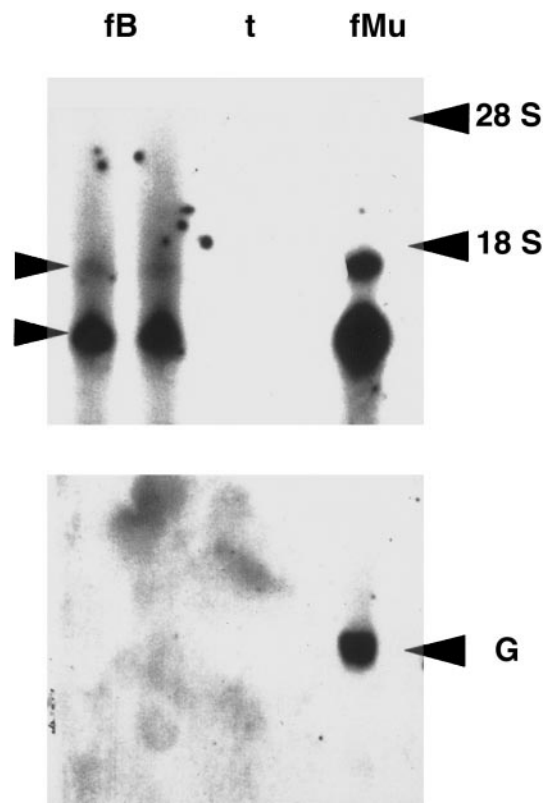

FIG. 9. (Upper panel) Northern blot analysis of 20 μg of self-hybridised and S1 nuclease-digested total RNA from foetal brain (fB) and 20 μg of yeast tRNA in comparison to 20 μg of undigested total RNA from foetal muscle (fMu). Total RNA from tissues were Northern blotted as either self-hybridised and digested (fB and t) or undigested RNAs (fMu) as described under Materials and Methods. The mitochondrial L-strand transcripts in the samples were detected with a ^{32}P end-labelled sense oligo (P4s) which spans the unusual assembly site of the RACE clone. Arrowheads on the right side indicate the position of the 28S and 18S rRNA in comparison to the specific mitochondrial L-strand transcripts. The estimated sizes of the L-strand transcript are approximately 800 nts and 1600 nts. (lower panel) The Northern blot was stripped and reprobed with an ^{32}P-labelled antisense cRNA specific for GAPDH RNA (G).

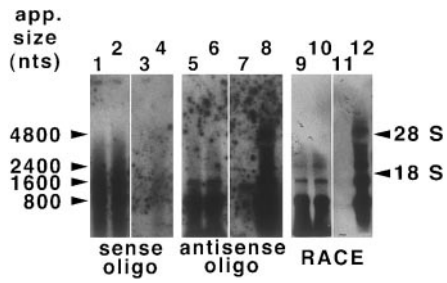

FIG. 10. Comparison of transcript sizes of the unusually assembled mitochondrial L- and H-strand RNAs by Northern blot analysis. Duplicates from 20 μg of self-hybridised and S1 nuclease-digested (see Materials and Methods) total RNA from porcine foetal brain (lanes 1, 2, 5, 6, 9, 10), 20 μg of yeast tRNA (lanes 3, 7, 11) and 20 μg of undigested total RNA from foetal brain (lanes 4, 8, 12) were analysed by Northern blotting with a ^{32}P end-labelled sense oligo (primer P4s) (lanes 1–4) and with a ^{32}P end-labelled antisense oligo (primer P4a) (lanes 5–8) which both span the unusual assembly site of the transcript, or with an antisense cRNA derived from the RACE clone (lanes 9–12). Arrowheads on the right side indicate the position of the 28S and 18S rRNA in comparison to the specific mitochondrial L- and H-strand transcripts. The estimated sizes of the L-strand transcripts, as indicated by the arrowheads, and numbers on the left side are approximately 800 and 1600 nts and of the H-strand transcript 800, 1600, 2400, and 4800 nts.

scripts of ATPase 6/8 and COIII are processed into individual RNAs without the punctuation signal of a tRNA gene. The fact that individual transcripts for the region of ATPase 6/8 and COIII exist demonstrates efficient processing of the polycistronic precursor RNAs without the need of a cleavage signal from interspersed tRNAs. Our data and the already reported unusual transcripts from the ATPase 6/8/COIII region (18) make this area of the mitochondrial genome an interesting spot to examine mitochondrial transcription and post-transcriptional events.

Our finding that the steady-state level of the H-strand transcript of the ATPase 6 region is upregulated in porcine brains during development (Figs. 1 and 4B) is in accordance with observations made during developmental changes in mitochondrial transcript levels of several species (26, 38–42); however, to our knowledge, the detection of a stable L-strand transcript (Figs. 2, 3, 4B) derived from this region has not yet been reported. According to the Northern blots, the sizes of the L- and the smallest H-strand transcripts are the same and represent the complete transcript length of the ATPase 6/8. A similar finding was reported by Tullo *et al.* (17), who detected an antisense transcript for the full length of the ND 6 mRNA which was more abundant than the actual coding RNA from. Although the relation of sense and antisense is different between ATPase 6/8 and ND 6 transcripts, the appearance of antisense transcripts, corresponding to coding regions of mitochondrial genes, might be a more general phenomenon in mitochondrial gene expression. It further demonstrates that the polycistronic L-strand transcript is processed to more stable RNAs than originally thought (43).

This L-strand transcript is detected in all tissues examined, except from foetal heart and is most pronounced in foetal brain (Fig. 3). Although the level of L-strand and H-strand expression cannot be compared directly, steady-state levels of the L-strand are definitely lower than those of the H-strand transcript. This is obvious from S1 nuclease protection assays, where signals from the L-strand transcript were detected in 20 μg of total RNA in most tissues only after 14 days of autoradiography, whereas respective H-strand signals were already visible within 14 h. Although we easily detected the H-strand transcripts in RNA from adult porcine brains by Northern blotting (Fig. 4B), the method was insufficient to provide evidence of the L-strand transcript in RNA from adult brains (data not shown), despite detection of the L-strand transcript in foetal tissue (Fig. 4B). The results show that the levels of L- and H-strand expression from adult and foetal brains are inverse to each other. There is a low level of H-strand expression in foetal brain and a high expression of this transcript in adult cerebrum and cerebellum (Figs. 1 and 4B); in contrast, the level of the L-strand transcript is higher in foetal brain than the steady-state level found in adult cerebrum and cerebellum (Figs. 2 and 3). It is well documented that nuclear and cytosolic factors affect mitochondrial gene expression (44–46) and vice versa, mitochondrial factors can influence nuclear and cytosolic events (47–49). Our results show for the first time a regulation of a mitochondrial L-strand transcript and the data suggest that developmental changes in the brain might regulate mitochondrial gene expression and could contribute to mitochondrial differentiation processes.

The mammalian mitochondrial genome almost exclusively consists of gene-coding sequences and, in contrast to the nuclear genome, does not contain intron sequences (8, 9). This lack of introns implies that mammalian mitochondrial gene expression would not require any splicosomal activity and thus makes the discovery of transcripts consisting of inversely assembled fragments most stunning. From the data presented in this manuscript (Figs. 9 and 10) we conclude that L- and H-strand transcripts have the same size. The fact that the unusually assembled H-strand transcript starts at the 5′ end with nt 8086 and ends at the 3′ site with nt 8085 suggested a circular structure of the original cDNA template, but so far PCRs with different combinations of primers have failed to prove a circularity. In Northern blottings all transcripts showed a size of approximately 800 bp or multiples thereof and thus it is improbable that the RACE clone represents the complete structure of the transcripts. The 5′ start of the unusually assembled transcript is most likely further upstream and the 3′ end further downstream. Whatever the complete structures of the

unusually assembled transcripts are, the already known sequences (Figs. 5A and 5B) make it unlikely that the transcripts contain a complete coding sequence for the ATPase 6 subunit. Therefore, it is not probable that the unusually assembled transcripts are translated into a functional ATPase 6 subunit.

Deletions at direct repeats in the mitochondrial genome are associated with a number of pathological processes in humans (e.g., Pearson and Kearns-Sayre syndromes) (50–54) and animals (55, 56). Mitochondria possess homologous DNA recombination activity (29), and recently a double strand break rejoining activity was discovered in mitochondrial extracts, which can cause deletions between direct repeats (30). In this context it is a remarkable feature of the unusually assembled transcript that the joined fragments overlap at a perfect 7 nts direct repeat. The experiments presented in the result section show that the unusually assembled transcripts are present in sense and antisense form and that they can build S1 nuclease-resistant double-stranded hybrids. In an earlier report, mitochondrial double-stranded RNAs were already described without assessing their function (57), but recently non-mitochondrial double-stranded RNAs were assigned as mediators in sequence specific genetic silencing and co-suppression [(58, 59) and references herein; for review, please see: (60)]. If the unusually assembled, double-stranded RNAs were transcribed from recombinant mitochondrial DNA, a significant portion of the mitochondrial genome would then contain the unusual sequence; but to our knowledge, so far such DNAs have not been reported. It is more likely that the RNAs are transcribed from normal mitochondrial DNA and that developmental specific mitochondrial-nuclear interactions cause the specific processing of the unusual transcripts.

The presented data for the expression of sense and antisense transcripts as well as the existence of the unusually assembled transcripts were demonstrated by several independent experiments, but up to now we can only speculate on the origin and possible physiological role(s) of these RNAs. Nevertheless, our results and the findings presented by other laboratories (17, 18) show that mitochondrial transcription and/or post-transcriptional processing are much more complex than currently recognised, and it should be taken into account that besides mitochondrial DNA mutations, abnormalities in mitochondrial RNA production and processing might also lead to pathological disturbances of mitochondrial gene expression.

ACKNOWLEDGMENTS

The authors thank Antje Isbrandt for kindly revising the manuscript. Part of the work was supported by the Verein zur Förderung von Forschung, Wissenschaft und Lehre an der Neurologischen Abteilung der Universitätsklinik in Göttingen.

REFERENCES

1. Parker, W. D., Jr., Parks, J., Filley, C. M., and Kleinschmidt-DeMasters, B. K. (1994) *Neurology* **44,** 1090–1096.
2. Beal, M. F. (1995) *Ann. Neurol.* **38,** 357–366.
3. Cassarino, D. S., and Bennett, J. P., Jr. (1999) *Brain Res. Brain Res. Rev.* **29,** 1–25.
4. Wallace, D. C., Singh, G., Lott, M. T., Hodge, J. A., Schurr, T. G., Lezza, A. M., Elsas, L. J. D., and Nikoskelainen, E. K. (1988) *Science* **242,** 1427–1430.
5. Holt, I. J., Harding, A. E., and Morgan-Hughes, J. A. (1988) *Nature* **331,** 717–719.
6. Howell, N. (1999) *Int. Rev. Cytol.* **186,** 49–116.
7. Cassarino, D. S., Parks, J. K., Parker, W. D., Jr., and Bennett, J. P., Jr. (1999) *Biochim. Biophys. Acta* **1453,** 49–62.
8. Attardi, G. (1985) *Int. Rev. Cytol.* **93,** 93–145.
9. Attardi, G., and Schatz, G. (1988) *Annu. Rev. Cell Biol.* **4,** 289–333.
10. Montoya, J., Christianson, T., Levens, D., Rabinowitz, M., and Attardi, G. (1982) *Proc. Natl. Acad. Sci. USA* **79,** 7195–7199.
11. Aloni, Y., and Attardi, G. (1971) *Proc. Natl. Acad. Sci. USA* **68,** 1757–1761.
12. Ojala, D., Montoya, J., and Attardi, G. (1981) *Nature* **290,** 470–474.
13. Montoya, J., Ojala, D., and Attardi, G. (1981) *Nature* **290,** 465–470.
14. Heddi, A., Lestienne, P., Wallace, D. C., and Stepien, G. (1993) *J. Biol. Chem.* **268,** 12156–12163.
15. Heddi, A., Lestienne, P., Wallace, D. C., and Stepien, G. (1994) *Biochim. Biophys. Acta* **1226,** 206–212.
16. Sbisa, E., Tullo, A., Nardelli, M., Tanzariello, F., and Saccone, C. (1992) *FEBS Lett.* **296,** 311–316.
17. Tullo, A., Tanzariello, F., D'Erchia, A. M., Nardelli, M., Papeo, P. A., Sbisa, E., and Saccone, C. (1994) *FEBS Lett.* **354,** 30–36.
18. Nardelli, M., Tommasi, S., D'Erchia, A. M., Tanzariello, F., Tullo, A., Primavera, A. T., De Lena, M., Sbisa, E., and Saccone, C. (1994) *FEBS Lett.* **344,** 10–14.
19. Cai, Q., and Storey, K. B. (1997) *Genome* **40,** 534–543.
20. Schiemann, S., Schwirzke, M., Brunner, N., and Weidle, U. H. (1998) *Clin. Exp. Metastasis* **16,** 129–139.
21. Wallenhorst, S., and Holtz, W. (1999) *J. Anim. Sci.*, in press.
22. Chirgwin, J. M., Przybyla, A. E., MacDonald, R. J., and Rutter, W. J. (1979) *Biochemistry* **18,** 5294–5299.
23. Liang, P., Averboukh, L., and Pardee, A. B. (1993) *Nucleic Acids Res.* **21,** 3269–3275.
24. Sambrook, J. F. E., and Maniatis, T. (1989) Molecular Cloning, Cold Spring Harbor Laboratory Press, New York.
25. Michel, U., Albiston, A., and Findlay, J. K. (1990) *Biochem. Biophys. Res. Commun.* **173,** 401–407.
26. Andreu, A. L., Arbos, M. A., Perez-Martos, A., Lopez-Perez, M. J., Asin, J., Lopez, N., Montoya, J., and Schwartz, S. (1998) *Biochem. Biophys. Res. Commun.* **252,** 577–581.
27. Anderson, S., Bankier, A. T., Barrell, B. G., de Bruijn, M. H., Coulson, A. R., Drouin, J., Eperon, I. C., Nierlich, D. P., Roe, B. A., Sanger, F., Schreier, P. H., Smith, A. J., Staden, R., and Young, I. G. (1981) *Nature* **290,** 457–465.
28. Vijayasarathy, C., Giger, U., Prociuk, U., Patterson, D. F., Breitschwerdt, E. B., and Avadhani, N. G. (1994) *Comp. Biochem. Physiol. A Physiol.* **109,** 887–894.
29. Thyagarajan, B., Padua, R. A., and Campbell, C. (1996) *J. Biol. Chem.* **271,** 27536–27543.

30. Lakshmipathy, U., and Campbell, C. (1999) *Nucleic Acids Res.* **27,** 1198–1204.
31. Montoya, J., Gaines, G. L., and Attardi, G. (1983) *Cell* **34,** 151–159.
32. Christianson, T. W., and Clayton, D. A. (1986) *Proc. Natl. Acad. Sci. USA* **83,** 6277–6281.
33. Christianson, T. W., and Clayton, D. A. (1988) *Mol. Cell Biol.* **8,** 4502–4509.
34. Attardi, G., Chomyn, A., Montoya, J., and Ojala, D. (1982) *Cytogenet. Cell Genet.* **32,** 85–98.
35. Chomyn, A., Mariottini, P., Gonzalez-Cadavid, N., Attardi, G., Strong, D. D., Trovato, D., Riley, M., and Doolittle, R. F. (1983) *Proc. Natl. Acad. Sci. USA* **80,** 5535–5539.
36. Mariottini, P., Chomyn, A., Attardi, G., Trovato, D., Strong, D. D., and Doolittle, R. F. (1983) *Cell* **32,** 1269–1277.
37. Fearnley, I. M., and Walker, J. E. (1986) *EMBO J.* **5,** 2003–2008.
38. Piko, L., and Taylor, K. D. (1987) *Dev. Biol.* **123,** 364–374.
39. Renis, M., Cantatore, P., Loguercio Polosa, P., Fracasso, F., and Gadaleta, M. N. (1989) *J. Neurochem.* **52,** 750–754.
40. el Meziane, A., Callen, J. C., and Mounolou, J. C. (1989) *EMBO J.* **8,** 1649–1655.
41. Marin-Garcia, J., Ananthakrishnan, R., Agrawal, N., and Goldenthal, M. J. (1994) *J. Mol. Cell Cardiol.* **26,** 1029–1036.
42. Chandramohan VA, H. W. (1999) *J. Biol. Chem.* **274,** 6265–6271.
43. Attardi, G., and Montoya, J. (1983) *Methods Enzymol.* **97,** 435–469.
44. Shan, B., Vazquez, E., and Lewis, J. A. (1990) *EMBO J.* **9,** 4307–4314.
45. Antonetti, D. A., Reynet, C., and Kahn, C. R. (1995) *J. Clin. Invest.* **95,** 1383–1388.
46. Enriquez, J. A., Fernandez-Silva, P., Garrido-Perez, N., Lopez-Perez, M. J., Perez-Martos, A., and Montoya, J. (1999) *Mol. Cell Biol.* **19,** 657–670.
47. Schulze-Osthoff, K., Krammer, P. H., and Droge, W. (1994) *EMBO J.* **13,** 4587–4596.
48. Maechler, P., Kennedy, E. D., Pozzan, T., and Wollheim, C. B. (1997) *EMBO J.* **16,** 3833–3841.
49. Hayakawa, T., Noda, M., Yasuda, K., Yorifuji, H., Taniguchi, S., Miwa, I., Sakura, H., Terauchi, Y., Hayashi, J., Sharp, G. W., Kanazawa, Y., Akanuma, Y., Yazaki, Y., and Kadowaki, T. (1998) *J. Biol. Chem.* **273,** 20300–20307.
50. Schon, E. A., Rizzuto, R., Moraes, C. T., Nakase, H., Zeviani, M., and DiMauro, S. (1989) *Science* **244,** 346–349.
51. Yuzaki, M., Ohkoshi, N., Kanazawa, I., Kagawa, Y., and Ohta, S. (1989) *Biochem. Biophys. Res. Commun.* **164,** 1352–1357.
52. Mita, S., Rizzuto, R., Moraes, C. T., Shanske, S., Arnaudo, E., Fabrizi, G. M., Koga, Y., DiMauro, S., and Schon, E. A. (1990) *Nucleic Acids Res.* **18,** 561–567.
53. Degoul, F., Nelson, I., Amselem, S., Romero, N., Obermaier-Kusser, B., Ponsot, G., Marsac, C., and Lestienne, P. (1991) *Nucleic Acids Res.* **19,** 493–496.
54. Zhang, C., Baumer, A., Maxwell, R. J., Linnane, A. W., and Nagley, P. (1992) *FEBS Lett.* **297,** 34–38.
55. Tanhauser, S. M., and Laipis, P. J. (1995) *J. Biol. Chem.* **270,** 24769–24775.
56. Van Tuyle, G. C., Gudikote, J. P., Hurt, V. R., Miller, B. B., and Moore, C. A. (1996) *Mutat. Res.* **349,** 95–107.
57. Harel, L., Riou, G., and Montagnier, L. (1975) *Biochimie* **57,** 227–233.
58. Sanchez Alvarado, A., and Newmark, P. A. (1999) *Proc. Natl. Acad. Sci. USA* **96,** 5049–5054.
59. Wargelius, A., Ellingsen, S., and Fjose, A. (1999) *Biochem. Biophys. Res. Commun.* **263,** 156–161.
60. Montgomery, M. K., and Fire, A. (1998) *Trends Genet.* **14,** 255–258.